Original Article

Prediction of Absorbed Dose to Normal Organs with Endocrine Tumors for I-131 by use of ^{99m}TC Single Photon Emission Computed Tomography/ Computed Tomography and Geant4 Application for Tomographic Emission Simulation

Rohollah Ghahraman Asl, Rezvan Sabbaghi[1], Hadi Taleshi Ahangari[1], Payman Hejazi[1], Majid Foroutan[2]

Department of Medical Physics and Radiation Sciences, Faculty of Paramedicine, Sabzevar University of Medical Sciences, Sabzevar, [1]Department of Medical Physics, Faculty of medicine, Semnan University of Medical Sciences, [2]Endocrinologist, Department of Internal Medicine, Faculty of Medicine, Semnan University of Medical Sciences, Semnan, Iran

Abstract

Introduction: This study aimed to predict the dose absorbed by normal organs with neuroendocrine tumors for ^{131}I using single photon emission computed tomography/computed tomography (SPECT/CT) images and Geant4 application for tomographic emission (GATE) simulation. **Materials and Methods:** Four to 5 whole-body planar scan series, along with one SPECT/CT image, were taken from four patients following ^{99m}Tc-hynic-Tyr^3-octreotide radiotracer injection. After image quantification, the residence time of each organ was calculated using the image analysis and the activity time curves. The energy deposit and dose conversion (S-value) were extracted from the GATE simulation for the target organs of each patient. Using the residence times and S-values, the mean absorbed dose for the target organs of each patient was calculated and compared with the data obtained from the standard method. **Results:** Very close agreement was obtained between the S-value of the self–organ irradiation. The mean percentage difference between the two methods (i.e. GATE and Medical Internal Radiation Dose [MIRD]) was 1.8%, while a weak agreement was observed for cross-organ irradiation. The percentage difference between the total absorbed doses by the organs was 2%. The percentage difference between the absorbed doses obtained for tumors and three considered normal organs estimated by the GATE method was slightly higher than the MIRD method (about 11% on average for tumors). **Conclusion:** Regardless of the small difference between the obtained results for the organs and absorbed doses of the tumors in the present study, patient-specific dosimetry by the GATE methods is useful and essential for therapeutic radionuclides such as ^{131}I due to high cross-dose effects, especially for young adult patients, to ensure the radiation safety and increase the effectiveness of the treatment.

Keywords: *Geant4 application for tomographic emission, I-131, image base internal dosimetry, patient-specific dosimetry, single photon emission computed tomography/computed tomography, S-value*

Introduction

Radionuclide therapy is a form of treatment, in which a systemic dose of a radioactive compound is administered to the patient to deliver the radionuclides to the tumors and damage their DNA. Compared with other treatment methods, the advantages of this method are the ability to directly transfer the radiation dose to the tumors and reduce the irradiation of normal tissues.[1-3] Owing to the ever-increasing application of radionuclides in medical diagnosis and treatment processes, a specific treatment protocol should be designed by assessing the absorbed dose to the tumors and normal tissues to maximize the dose administered to the tumors and minimize the dose absorbed by the normal tissues.[4] In the therapeutic processes, widely used radionuclides such as I-131 can be used for the treatment of thyroid disease, Ra-223 for relieving and treatment of bone tumors, Lu-177 for the treatment of neuroendocrine tumors, and Y-90 for radioembolization. In addition, radionuclides such as Tc-99m, I-123, and Tl-201 can be used in diagnostic processes.[5-8] One of the principal quantities in patient-specific dosimetry calculations is the absorbed dose, which is defined as the energy absorbed per unit mass of the interested tissue. The absorbed dose is

How to cite this article: Asl RG, Sabbaghi R, Ahangari HT, Hejazi P, Foroutan M. Prediction of Absorbed Dose to Normal Organs with Endocrine Tumors for I-131 by use of 99mTC Single Photon Emission Computed Tomography/ Computed Tomography and Geant4 Application for Tomographic Emission Simulation. Indian J Nucl Med 2021;36:273-81.

Address for correspondence:
Dr. Hadi Taleshi Ahangari, Department of Medical Physics, Faculty of Medicine, Semnan University of Medical Sciences, Semnan, Iran.
E-mail: taleshi@semums.ac.ir

Received: 16-01-2021
Revised: 30-04-2021
Accepted: 07-05-2021
Published: 23-09-2021

Access this article online

Website: www.ijnm.in
DOI: 10.4103/ijnm.ijnm_6_21
Quick Response Code:

influenced by several factors, including the physical and biological half-life of the radiopharmaceutical, the amount of activity administration, the energy and frequency of the radiation emitted from the source organ, and the amount absorbed in the target organ. This quantity is dependent on the shape, composition, and location of the target organ.[9]

Biomedical half-life requires evaluating the biological distribution of radiopharmaceuticals in the body, which can be obtained through imaging techniques such as positron emission tomography (PET), single photon emission computed tomography (SPECT), or planar scintigraphy. Furthermore, the shape and information regarding the structure of the target regions could be acquired through anatomical imaging modalities such as computed tomography (CT) and magnetic resonance imaging.[10] One of the most common methods of calculating the dose absorbed by the patient is using the dose conversion factor (i.e. S-value) and the proposed formulation of the internal medicine dosing committee in nuclear medicine (i.e. Medical Internal Radiation Dose [MIRD]).[11] Researchers have identified various programs, such as the MIRDOSE program (or its higher version, OLINDA), for internal dosimetry according to standard phantoms in diagnostic and therapeutic processes based on pre-calculated S-values.[12,13] The MIRDOSE program uses Cristy-Eckermans reference male and female phantoms to calculate the S-values and the mean absorbed dose of the target organs at the organ level for different radionuclides.[14] In the standard method, the activity distribution in the source organ is considered uniform, and the dose is uniformly deposited throughout the target organ. However, the evidence indicates that in the case of radionuclides, specifically in therapeutic types, the biological effects of tumor response and the toxicity of normal tissues are not properly predicted by the mean absorbed dose. Moreover, the standard phantom approach is not suitable to calculate the dose absorbed by the tumors, where the anatomy of the patient's normal organs is affected by the tumor size, shape, and position in the patient. In fact, although the self-dose of tumors can be calculated as an example, the distribution of tumor doses from other source organs of the body cannot be calculated, which is unlikely for radionuclides with high energy photons such as I-131.[15-17]

The development of hybrid imaging technologies, such as PET/CT and SPECT/CT, increased the capability of performing patient-specific dosimetry diagnosis and therapy using radionuclides by providing spatial and temporal distribution of activity with anatomical information.[18-20] Furthermore, in base Monte Carlo methods, it is now possible to consider the precise geometry of the source and target organs, as well as the heterogeneities of tissues within the body for each patient, with the help of scintigraphy and anatomical images.[21] On the other hand, the patient-specific dosimetry obtained from the images of the patients, along with Monte Carlo calculations, is not only useful for optimizing the prescribed activities and increasing therapeutic efficiency but also they could also be employed for creating the minimum-effective dose and determining the dose-response relationship as a basis for predicting clinical results.[22] The examples of Monte Carlo codes, which are commonly employed in nuclear medicine and radiotherapy applications, include the EGS,[23] MCNP,[24] and GEANT.[25,26] Geant4 Application for Tomographic Emission (GATE)[27] is a simulation code based on GEANT4,[25] dedicated mainly to nuclear medicine processes. The reliability of this code is appropriate due to better physical interaction and more validity.[28]

Therefore, our goal in this study is to predict the dose absorbed by normal organs with neuroendocrine tumors for I-131 using SPECT/CT images and GATE simulation. To analyze the GATE simulation method and assess the accuracy of dose calculations based on the patient images, the results were compared with the most common tool in this field.

Materials and Methods

Imaging of patients

A total of four patients, including two males and two females, suspected of having neuroendocrine tumors, were evaluated with ^{99m}Tc-hynic-Tyr^3-octreotide imaging. The demography of the patients, including their organ mass, is listed in Table 1. In addition, MIRD standard phantom data are available for comparison. After injecting each patient with approximately 20–25 mCi of the radiotracer, four to five whole-body scans were obtained over a period of 1–24 h (time points = 1, 2, 5, 6, and 20 h). The imaging was a Siemens device with a dual-head gamma camera (made in the USA) and a low-energy high-resolution collimator. Whole-body anterior (I_A) and posterior (I_p) views were obtained according to the routing protocol employed in the clinic, including a 256×1024 matrix with a pixel size of 4.79 mm and a scan speed of 20 cm/min. Furthermore, a SPECT scan was taken over 180° (circular orbit) in 64 view/head and 20 S-frame and was recorded in a 128×128 matrix. CT scans were obtained before the SPECT scan, with a 512×512 matrix size using a tube voltage of 130 kV and a tube current of 25 mA to create attenuation maps and measure the body diameter and internal organ boundaries.

Quantification of patients' images

After reconstructing the images using the Ordered Subset Expectation Maximization algorithm, isocontours were drawn in the reconstructed images with a 40% threshold, and the count density values in the source and target organs were obtained for all patients.[29] A triple-energy window technique was also employed to estimate the scatter. The width of the photo-peak window was 15%, whereas the widths of the upper and lower scattered windows were 7%.

Table 1: Demographic information of 4 patients with information on medical internal radiation dose phantom and organ selective mass

	Patients and phantoms characteristics				Organ masses			
	Sex	Age (years)	Weight (kg)	Height (cm)	Kidneys	Liver	Spleen	Thyroid
Patient 1	Male	27	61	164	220.3	1315.4	395.4	18
Patient 2	Male	42	84	179	308.6	2239.9	306.7	25
Patient 3	Female	64	73	155	266.1	1245.1	214.2	20
Patient 4	Female	63	53	158	280.4	1284.0	357.8	16
MIRD adult phantom	Male	-	73.7	167	299.0	1910.0	183.0	20
MIRD adult phantom	Female	-	56.8	157	255.0	1400.0	150.0	17

MIRD: Medical internal radiation dose

To rectify the attenuation in the target volume of interest, based on the effective attenuation coefficient (μ-value = 0.15 cm^{-1}) obtained from CT images, MIRD was employed according to pamphlet No. 16.[30] To acquire the gamma camera calibration factor (K) necessary for absolute quantification, a planar scan is taken from a point source with activity A in the air, followed by measuring the count rate by summing the values of Y counts over a period of time (d).[31] The unit for K is cpm/MBq.

$K = Y/A.d$ (Equation 1)

Using Equation 2, the absolute activity in the source and target organs was calculated by correcting the counts in the volumes of interest and dividing the result by the camera calibration factor.

$$A(j) = \frac{R_0(j)}{K} = \frac{R_{corr}(j)}{K.T}.f \quad \text{(Equation 2)}$$

Where $R_{Corr\ (j)}$ is the count rate corrected in the volumes of interest and *f* is the self-absorption correction factor in the source organ. ($f = [(\mu jdj/2)/\sinh(\mu jdj/2)]$) where μj and *dj* are the source region attenuation coefficient and source thickness, respectively. The transmission factor for the patients can be calculated using the diameter of their body and the tissue linear absorption coefficient.

Calculation and plot of time activity curves

A hybrid planar/SPECT approach was used to plot the time-activity curves. The first image from the whole-body scans of each patient was selected, and regions with significant uptake were manually drawn around each tumor, where normal organs included the kidneys, liver, thyroid, and spleen. Regions of Interest (ROIs) were created automatically by applying a threshold of 40% to the maximum pixel counts to be used in the clinical practice. These two-dimensional ROIs were then manually registered in the data from the corresponding regions in the remaining whole-body scans at the following time points. After background correction for anterior and posterior images, the mean value for the corrected counts (i.e. $(I_A I_P)^{1/2}$) was employed to obtain the time-counts curve. The planar image was used to determine the effective elimination constant (λ_{eff}). Then, using Equation 3, the effective half-life of the region was calculated. By scaling each curve based on the activity calculated from the SPECT (ASPECT) images at the time of imaging (tSPECT), the cumulated activity (Ã) was determined according to Equation 4.

$T_{eff} = Ln\ (2)/\lambda_{eff}$ (Equation 3)

$A = A_{SPECT}\ (\exp\ (\lambda_{eff}\ t_{SPECT})/\lambda_{eff})$ (Equation 4)

Predicted time-integrated activity coefficients (TIACs) were calculated for ^{131}I by assuming a pharmaceutical labeled with the same radionuclides. These coefficients would follow similar time-dependent bio-distribution as the ^{99m}Tc labeled tracer. According to the following equation, the I-131 cumulated activity was corrected due to the difference in the physical half-life of the imaging and treatment radioisotope.[32]

$$A_{131I} = A_{99mTc} e^{(\lambda_{99mTc} - \lambda_{131I})t} \quad \text{(Equation 5)}$$

In this equation, λ_{99mTc} (= Ln (2)/6) is the physical decay constant of the ^{99m}Tc, (= Ln (2)/192.5) is the physical decay constant for ^{131}I, and t is the SPECT imaging time. The residence time required to calculate the absorbed dose on the organ scale is obtained by dividing the cumulated activity by the injected activity for each source organ.

Calculating the absorbed dose with MIRDOSE software

The MIRD formulation has been proposed by the MIRD Committee and is widely accepted for organ absorbed dose calculations.[33] Based on this formulation, the energy deposited from the source organ to the target organ is obtained using the residence time determined from scintigraphy images. The MIRDOSE program Version 3.1 Michael Stabin (PhD) wrote the MIRDOSE 3.0 and 3.1. MIRDOSE was relied upon for a number of years and was been used by thousands of medical, safety, and regulatory professionals was used to calculate the mean absorbed dose in different organs of the patient in terms of mGy/MBq. In addition, this program includes S-value tables for radionuclides and various standard phantoms in terms of mGy/MBq-s. By entering the residence time for the target organs, selecting ^{131}I radionuclide, and selecting the female or male reference phantom, the mean absorbed dose is calculated using precalculated S-value, and the absorbed dose is calculated using Equation 6.

$$D(r_k) = \sum_{r_h} A_{r_h} S(r_k \leftarrow r_h) \quad \text{(Equation 6)}$$

In this equation, r_k is the target organ, r_h is the source organ, and $\tilde{A}_{rh}$ is the time-cumulated activity in the source organ. The mean absorbed dose of the target organ included the self and cross-doses.

Calculate the absorbed dose with the Monte Carlo computational code

The GATE Monte Carlo method is based on GEANT4 library data[25] for radiation transport calculations. GATE is the only proprietary code available in the field of nuclear medicine that includes the items of dose distribution in the body.[34] This method was employed to estimate the absorbed dose of patients on the voxel level. In this method, all patient input files are converted to the interfile format, which is an acceptable format for GATE. A set of SPECT/CT fused images of patients with matrix dimensions of 128×128 and voxel dimensions of 4.79 mm ×4.79 mm ×4.79 mm were employed to define the geometry, attenuation map, and spatial distribution of the radiotracer. Approximately 100 million particles were tracked in each period of the calculations, and finally, an absorbed dose and a set of dose conversion factors were obtained for each pair of source and target organs.

Estimated absorbed dose assessment

The estimation for the absorbed dose was performed using the MIRDOSE. Moreover, the GATE computational method was carried out using the comparison of S-value and comparing the total absorbed dose of target organs and tumors.

Comparing S-values

Based on standard MIRD phantoms and patient-specific images, the S-values of MIRDOSE were compared with the S-values of GATE in the GATE Monte Carlo method to determine the percentage of relative difference (%RD). The mass correction of S-values was performed to resolve the mass difference between the organs of patients and standard phantoms.

$$\%RD = \frac{S_{MIRDOSE}(r_T \leftarrow r_s) - S_{GATE}(r_T \leftarrow r_s)}{S_{GATE}(r_T \leftarrow r_s)} \times 100 \quad \text{(Equation 7)}$$

It is noteworthy that the results obtained from the MIRD method were considered as reference data.

Comparing the total absorbed dose reached by the organs

It is noteworthy that the results obtained from the MIRD method were considered as the reference data. Moreover, the mean absorbed dose by normal and tumor organs, obtained from GATE and MIRD for more accurate assessment, were compared, and the percentage difference between the two methods was obtained. Furthermore, self and cross-dose contributions of each organ were considered in comparison with tumor dose and normal organs. It should be noted that the tumor dose in the MIRD method is calculated using the sphere model and includes the self-dose only.

Results

Time activity curves

As can be seen in Table 1, although the height and weight of some patients were close to the MIRD phantom, the mass of their organs was different. Typical examples of organ time–activity curves obtained from planar images of the right kidney, liver, thyroid, and spleen for the four patients are demonstrated in Figure 1. Moreover, the residence time obtained from the quantification of planar and tomographic images for the source organs of these four patients is listed in Table 2.

The percentage relative difference between S-values from the GATE and MIRD methods for each pair of source and target organs are expressed in Table 3. The mass correction was performed for GATE method data, and it was compared with the data from the MIRD. As can be seen, the agreement between cross-absorbed *S-value*s (i.e. when the source and target organs are different) in GATE and MIRD was very poor (ranging from − 43.8% to 78.6%). However, a very close agreement was obtained between self-absorbed *S-value*s (i.e. when the source organ and the target are the same) with an average percentage difference of 1.8%. These discrepancy values for ^{131}I were in agreement with the values reported by Grimes and Celler.[35] As can be seen in that study, they evaluated six patients undergoing whole-body and tomographic imaging and employed the TIACs as the input of the OLINDA program to determine the dose of the organs. Also, the predicted residence times for ^{131}I and ^{177}Lu were assumed for the radiopharmaceuticals labeled with these radionuclides following the biological distribution of the ^{99m}Tc radiotracer time. For ^{131}I radionuclide, they reported a mean difference percentage of 2.3% for self-absorbed, and the S-value difference ranges from − 38% to 105% for cross-adsorbed between EGSnrc and MIRD method. In our study, the determined mean percentage difference of S-values between GATE and MIRD for self-organ irradiation included S (spleen ← spleen), S (Thyroid ← Thyroid), S (kidney ← kidney), and S (liver ← liver), respectively, and was equal to − 0.48, 0.2, 3.52, and − 3.72 (on average − 1.88). It is also noteworthy that in the study

Table 2: Residence times of the selected source organs in this study

	Residence times (h)			
Organ	**Patient 1**	**Patient 2**	**Patient 3**	**Patient 4**
Kidneys	0.28	0.2	0.38	0.39
Liver	0.79	0.5	1.26	1.81
Spleen	1.81	0.3	0.6	1.85
Tumor	-	0.06	0.22	0.05
Thyroid	0.013	0.019	0.017	0.03

of Momennezhad *et al*.,[18] the values reported for self-organ irradiation of spleen, liver, and kidneys for ^{99m}Tc radionuclide were − 6.3, 3.8, and − 0.5%, respectively.

The total dose of tumors and normal organs

In order to provide a more accurate comparison between the results, the total dose of GATE and MIRD methods for the four target organs (i.e. liver, kidney, thyroid, and spleen), as well as a tumor with absorbed dose ratios in the two methods are listed in Table 4. The mean dose absorbed by the normal organs of the patients for the target organs was estimated to be 0.15, 0.11, 0.43, and 0.13 mGyMBq, respectively.

Figure 2 illustrates the GATE to MIRD absorbed dose ratio for the four mentioned organs in all patients. Based on this Figure, the estimated absorbed dose by the GATE method for spleen tissue in patients 2 and 4, liver tissue in patient

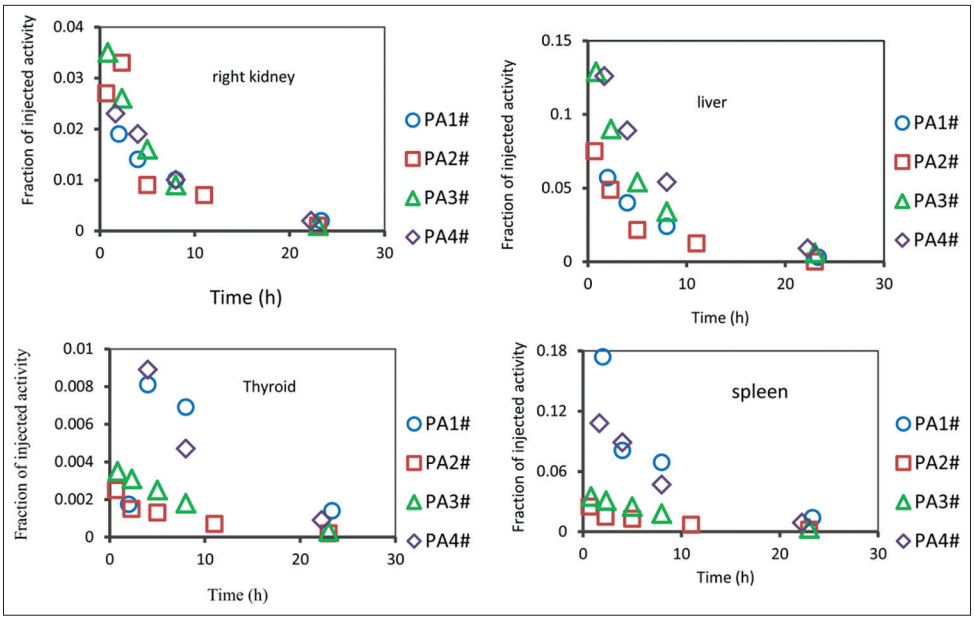

Figure 1: Decay time activity data for some of the normal organs of the four patients

Table 3: Summary of percentage differences between ^{131}I patient-specific *S* values (mGy/MBq.s) calculated by GATE and MIRD methods for 4 patients

Percentage RD	Patient 1				Patient 2				Patient 3				Patient 4			
	K	S	L	T	K	S	L	T	K	S	L	T	K	S	L	T
Kidneys	-6.8	9.7	47.6	78.6	-4.2	-37.8	-10.8	-21.7	-5.5	-7	-86	16	2.4	-19.4	-39.3	-32.8
Spleen	10	-1	64.5	-31.9	-37.3	-1	46.3	-21.9	-6.2	3.4	-1.9	25.6	-18.5	0.5	60.9	4.7
Liver	18.7	66.4	-5.8	30.4	-13	45.8	-1.4	28.9	-39.3	-2.2	-4.2	-23.8	-39.3	59.6	-3.5	-2
Thyroid	61.4	-28.7	30.4	1.3	-43.8	-25.2	-30.4	0.6	15.8	27.9	-23.2	0.5	-29	5.2	-2.2	-1.6

K: Kidney, L: Liver, S: Spleen, T: Thyroid, RD: Relative difference

Table 4: Organ dose calculatedfor131I by GATE and medical internal radiation dose methods

	Total dose (self-dose+cross-dose) (mGy/MBq)							
	Kidneys		Liver		Thyroid		Spleen	
	GATE	MIRD	GATE	MIRD	GATE	MIRD	GATE	MIRD
Patient 1	1.39E-1	1.80E-1	8.54E-2	9.03E-2	7.50E-2	7.36E-2	5.76E-1	5.83E-1
Ratio D_{GATE}/D_{MIRD}	0.77		0.94		1.02		0.99	
Patient 2	8.01E-2	8.48E-2	3.50E-2	3.33E-2	1.14E-1	1.07E-2	1.30E-1	1.25E-1
Ratio D_{GATE}/D_{MIRD}	0.94		1.05		1.06		1.04	
Patient 3	1.82E-1	1.88E-1	1.41E-1	1.46E-1	1.21E-1	1.17E-1	3.45E-1	3.56E-1
Ratio D_{GATE}/D_{MIRD}	0.97		0.97		1.03		0.97	
Patient 4	1.88E-1	1.95E-1	1.97E-1	2.04E-1	2.03E-1	2.06E-1	6.64E-1	6.53E-1
Ratio D_{GATE}/D_{MIRD}	0.96		0.96		0.98		1.02	
Total dose (GATE)	1.47E-1		1.15E-1		1.28E-1		4.26E-1	

MIRD: Medical internal radiation dose, GATE: Geant4 application for tomographic emission

2, and thyroid tissue in patients 2, 1, and 3 were higher than the MIRD method. The mean ratio of the adsorbed doses estimated by GATE and MIRD for all organs of the studied patients was 0.99, with a difference ranging from 0.77 to 1.06. The lowest agreement is related to the dose adsorbed by the kidney tissue in patient 1.

The values for tumor mass and the estimated adsorbed dose for the tumors of the considered patients are listed in Table 5 using GATE and MIRD methods. As can be seen, there is a significant difference between the total dose absorbed by the tumor in the two methods studied. However, a good agreement in self-dose was calculated between GATE and MIRD methods with an average difference of 3%. The mean relative difference percentage of total tumor dose calculated by the GATE method and MIRDOSE nodule module was 11% following mass correction, which is in agreement with the study by Grimes and Celler[35] In that study, the error percentage was reported as − 3.5% for self-absorbed and − 6% for total dose. The negative sign in the error percentages in this study was due to the subtraction of the calculated data with the MCNP code from MIRD data. On the contrary, the error percentage in the present study is obtained by subtracting GATE data from MIRD, and thus, is positive.

Figure 3 illustrates the contribution of self-dose and cross-dose to the tissues of the kidneys, liver, thyroid, and spleen. The highest absorbed dose was related to the thyroid self-dose due to its remoteness from other organs. Since the cross-dose is fundamentally dependent on the distance between the organs, more than 90% of the total dose in all organs is self-dose. This value was in agreement with the study by Rajendran *et al*.[37]

In Sandström *et al*.[38] study, the contribution of cross-dose in the total dose was 2% for the kidneys of most patients, and it was less than 10% for ^{177}Lu radionuclide in almost all patients. It is worth mentioning that in our study, the contribution of the cross-dose for ^{131}I radionuclide was 10%, which was higher than ^{177}Lu. This difference can be related to the gamma-ray energy of 364 kV emitted by ^{131}I with a higher probability (82%) in comparison with the gamma-ray energy of 113 and 208 kV, with a respective probability of 6.4 and 11% for ^{177}Lu. In specific, lower energy photons deposit more energy to their neighboring source organs, while higher energy photons are less attenuated and more likely to deposit their energy to the target organs, which are farther from the source organs.

Discussion

In this study, the adsorbed dose and the dose conversion factors for source and target organs of the four patients were obtained using specific images. In general, there was a very close agreement between the total organ dose from the GATE and MIRD methods. Therefore, the relative percentage difference between the total dose for the patients in this study was 2% using two methods. As can be deduced from the study by Sgouros *et al*.,[36] the percentage difference in the mean dose absorbed by the 15 patients treated with ^{131}I was reported between 2% and 5%, which was acquired with the help of the 3D-ID program and the standard MIRD method. However, the percentage difference in S-value in the cross-organ irradiation was

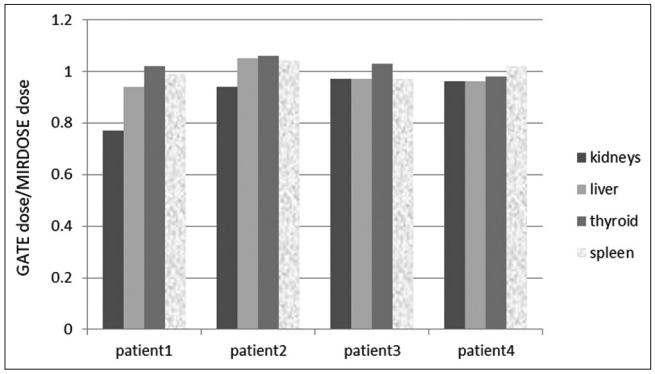

Figure 2: Ratio between Geant4 application for tomographic emission and MIRDOSE absorbed doses for the four patients. No tumor was visible in a single single photon emission computed tomography field of view for patient 1

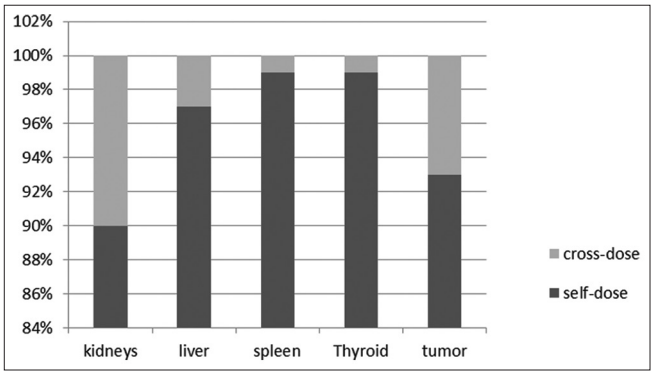

Figure 3: The percent contributions of self- and cross-doses

Table 5: Tumor mass, tumor doses for patients with pathologic uptake

	Patient 1		Patient 2		Patient 3		Patient 4	
Tumor numbered	-		2		1		1	
Tumor mass (g)	-		47.54		24.45		18.08	
	GATE	MIRD	GATE	MIRD	GATE	MIRD	GATE	MIRD
Self-dose (GATE)	-	-	6.36E-01	5.72E-01	1.01E+00	1.02E+00	2.89E-01	2.96E-01
Total dose	-	-	6.42E-01	5.67E-01	1.014E+00	1.02E+00	3.53E-01	2.96E-01

MIRD: Medical internal radiation dose, GATE: Geant4 application for tomographic emission

weak in our study. Nonetheless, the detected relative difference in S-value was between − 43.8% and 78.6%, which was in agreement with the reported range differences in the studies by Divoli *et al*.[39] and Momennezhad *et al*.[18] The S-value relative difference in the cross-organ irradiation in the study of Momennezhad *et al*.[18] for ^{99m}Tc radionuclide with GATE method and MIRDOSE program ranged from −28.9% to 98%. Moreover, in Divoli *et al*.,[39] the S-value of ^{131}I radionuclide with MCNP code and MIRDOSE program has been reported between −51% and 84%. Reviewing the absorbed dose values in our study indicates that the contribution of cross-doses was about 10% of the total dose, and the highest contribution was related to the self-dose. However, there was a good agreement between the total dose of GATE and MIRD for the target organs of the patients.

In addition, Table 5 shows a significant difference between the dose absorbed by the tumor in the two methods employed. The mean difference percentage between the total dose of the tumor (including self- and cross-dose) by GATE and MIRDOSE program (using the sphere model) was equal to 11% following mass correction. This difference is due to the fact that the determined dose absorbed by the tumors in the MIRDOSE program is less than the GATE. Another reason for this percentage error is that the contribution of the cross-irradiation was considered in the GATE method, while the MIRDOSE program is incapable of determining this contribution. Compared to the Grimes and Celler[35] study, this difference was lower by approximately 6%, which could be related to the difference in the volume of tumors examined (23 to 95 g compared to 18 to 47.5 g in the present study).

As shown in Table 4, the mean total dose per unit (mGy/MBq) for kidneys, liver, spleen, and thyroid is 0.15, 0.11, 0.43, and 0.13, respectively. Analyzing the data from the patients confirmed that the dose absorbed by the spleen organ in patients 1 and 4 were lower than patients 2 and 3 with higher organ mass, and the dose absorbed by the liver in patients 1 and 2 were lower with higher body mass.

The reason for this is the inverse relationship between the mass and dose conversion factors and the absorbed dose. These values were in agreement with the Pandit-Taskar *et al*.[40] study. They estimated the dose absorbed by the organs of 33 patients treated with the^{131}I-MIBG, which were obtained from three whole-body planar scans over a period of 2–6 days. Moreover, the dose absorbed by 14 organs was calculated using the OLINDA program. The absorbed dose by kidneys, liver, spleen, and thyroid was reported as 0.16, 0.48, 0.16, and 0.156, respectively. Similar results have been reported by Kolbert *et al*.[41]

The mean total dose for thyroid cancer patients treated with ^{131}I source using the 3D-ID program for the right kidney, left kidney, liver, and spleen was 0.095, 0.1, 0.094, and 0.087, respectively. The estimated doses mentioned in the two studies for the organs and the present study were close to each other with acceptable uncertainty.

In fact, the actual weight of the patients, the size of their body organs, and the distance between the organs differ significantly from the volumes and distances described in the standard models. For example, the size of the spleen in adult patients varies from approximately 50 to 600 g, while the size of the spleen in the standard adult MIRD phantom is 183 g.

The absorbed dose by the organ is inversely proportional to its mass. Therefore, it can be concluded that the difference in the dose absorbed by the liver and kidney in the present study, and the study by Pandit-Taskar *et al*.[40], may be due to the use of phantom-based models to estimate the absorbed dose. In another study,[42] the mean dose absorbed by the liver and spleen was 0.21 and 0.47 (mGy/MBq) using the 3D-ID program.

In another similar study, during the ^{99m}Tc[18] imaging with the GATE method for the kidneys, liver, and spleen, the dose absorbed was 0.021, 0.012, and 0.03 mGy/MBq, respectively. Therefore, it is concluded that the difference in radionuclide type can provide different dosimetric results since the results of the ^{99m}Tc dosimetry are less than those of the ^{131}I. However, due to the limitations and unavailability of thyroid cancer patients treated with low-prescribed activity values of iodine-131, along with the problems related to the iodine-131 image quantification, in this study, ^{99m}Tc-hynic-Tyr^3-octreotide images were employed to investigate the biological distribution of radionuclide in bodies of the patients. Nevertheless, the obtained results are close to similar studies with acceptable uncertainty.

Conclusion

Patient-specific internal dosimetry, using the GATE Monte Carlo program and based on a series of planar images and SPECT/CT images of the patient, contains various information, including tissue heterogeneities, nonuniformity of the activity distribution, and the actual geometry of the source and target organs in each patient. Despite the small differences between the obtained results of the doses absorbed by the organs and tumors in the present study, patient-specific dosimetry using the GATE method is useful and important for therapeutic radionuclides such as ^{131}I due to high cross-dose effects, especially for young adult patients, to ensure the radiation safety and increase the effectiveness of treatment.

Acknowledgment

This work was performed in partial fulfillment of the requirements for Msc of Rezvan Sabbaghi, in faculty of medicine, Semnan University of Medical Sciences, Semnan, Iran.

This article is an excerpt from the thesis research project approved at Sabzevar University of Medical Sciences and

Semnan University of Medical Sciences with the code of ethics IR.MEDSAB.REC.1397.147 and IR.SEMUMS.REC.1397.147. In this way, the authors express their gratitude and appreciation for the financial support of the research assistants of both universities.

Financial support and sponsorship

The authors gratefully acknowledge the Research Council of Sabzevar University of Medical Sciences and Semnan University of Medical Sciences for financial support.

Conflicts of interest

There are no conflicts of interest.

References

1. Davies AJ. Radioimmunotherapy for B-cell lymphoma: Y90 ibritumomab tiuxetan and I (131) tositumomab. Oncogene 2007;26:3614-28.
2. Bednarz B, Besemer A. Radiation-Induced Second Cancer Risk Estimates From Radionuclide Therapy. InEPJ Web of Conferences 2017 (Vol. 153, p. 04020). EDP Sciences. Available from: https://doi.org/10.1051/epjconf/201715304020. [Last accessed 2021 May 31].
3. Gallivanone F, Valente M, Savi A, Canevari C, Castiglioni I. Targeted radionuclide therapy: Frontiers in theranostics. Front Biosci (Landmark Ed) 2017;22:1750-9.
4. Li T, Zhu L, Lu Z, Song N, Lin KH, Mok GS. BIGDOSE: Software for 3D personalized targeted radionuclide therapy dosimetry. Quant Imaging Med Surg 2020;10:160-70.
5. Li T, Ao EC, Lambert B, Brans B, Vandenberghe S, Mok GS. Quantitative imaging for targeted radionuclide therapy dosimetry – Technical review. Theranostics 2017;7:4551-65.
6. Vente MA, Nijsen JF, de Roos R, van Steenbergen MJ, Kaaijk C, Koster-Ammerlaan MJ, *et al.* Neutron activation of holmium poly (L-lactic acid) microspheres for hepatic arterial radioembolization: A validation study. Biomed Microdevices 2009;11:763-72.
7. Yeong CH, Cheng MH, Ng KH. Therapeutic radionuclides in nuclear medicine: Current and future prospects. J Zhejiang Univ Sci B 2014;15:845-63.
8. Bardiès M. Relevance and implementation of patient-specific dosimetry in targeted radionuclide therapy. InBIO Web of Conferences 2019 (Vol. 14, p. 07001). EDP Sciences. Available from: https://doi.org/10.1051/bioconf/20191407001. [Last accessed 2021 May 31].
9. Saha GB. Physics and Radiobiology of Nuclear Medicine. 4rd ed. New York: Springer Science and Business Media; 2012.
10. Pérez P, Valente M. DOSIS: An integrated computational tool for patient-specific dosimetry in nuclear medicine by Monte Carlo and dose point kernel approaches. Appl Radiat Isot 2019;150:135-40.
11. Bolch WE, Bouchet LG, Robertson JS, Wessels BW, Siegel JA, Howell RW, *et al.* MIRD pamphlet No. 17: The dosimetry of nonuniform activity distributions – Radionuclide S values at the voxel level. Medical Internal Radiation Dose Committee. J Nucl Med 1999;40:11S-36.
12. Stabin MG, Sparks RB, Crowe E. OLINDA/EXM: The second-generation personal computer software for internal dose assessment in nuclear medicine. J Nucl Med 2005;46:1023-7.
13. Stabin MG. MIRDOSE: Personal computer software for internal dose assessment in nuclear medicine. J Nucl Med 1996;37:538-46.
14. Gorji KE, Firouzjah RA, Khanzadeh F, Abdi-Goushbolagh N, Banaei A, Ataei G. Estimating the absorbed dose of organs in pediatric imaging of 99mTc-DTPA radiopharmaceutical using MIRDOSE software. JBPE 2019;9:285-94.
15. Ljungberg M, Sjögreen-Gleisner K. The accuracy of absorbed dose estimates in tumours determined by quantitative SPECT: A Monte Carlo study. Acta Oncol 2011;50:981-9.
16. Bailey DL, Hennessy TM, Willowson KP, Henry EC, Chan DL, Aslani A, *et al. In vivo* quantification of (177) Lu with planar whole-body and SPECT/CT gamma camera imaging. EJNMMI Phys 2015;2:20.
17. O'Donoghue JA. Implications of nonuniform tumor doses for radioimmunotherapy. J Nucl Med 1999;40:1337-41.
18. Momennezhad M, Nasseri S, Zakavi SR, Parach AA, Ghorbani M, Asl RG. A 3D Monte Carlo method for estimation of patient-specific internal organs absorbed dose for 99mTc-hynic-Tyr3-octreotide imaging. World J Nucl Med 2016;15:114-23.
19. Lyra M, Lagopati N, Charalambatou P, Vamvakas I. Patient-specific dosimetry in radionuclide therapy. Radiat Prot Dosimetry 2011;147:258-63.
20. Bagheri M, Parach AA, Razavi-Ratki SK, Nafisi-Moghadam R, Jelodari MA. Patient-specific dosimetry for pediatric imaging of 99mTc-dimercaptosuccinic acid with gate Monte Carlo code. Radiat Prot Dosimetry 2018;178:213-22.
21. Huizing DM, de Wit-van der Veen BJ, Verheij M, Stokkel MP. Dosimetry methods and clinical applications in peptide receptor radionuclide therapy for neuroendocrine tumours: A literature review. EJNMMI Res 2018;8:89.
22. Canzi C, Traino AC. Dosimetry in the radioiodine treatment of hyperthyroidism. In: Bombardieri E, Seregni E, Evangelista L, Chiesa C, Chiti A, editors. Clinical Applications of Nuclear Medicine Targeted Therapy. Cham: Springer International Publishing; 2018. p. 33-44.
23. Rogers D. Low energy electron transport with EGS. Nucl Instrum Meth A 1984;227:535-48.
24. Hendricks J, Briesmeister J. Recent MCNP developments. IEEE T Nucl Sci 1992;39:1035-40.
25. Pia MG. The Geant4 Toolkit: Simulation capabilities and application results. Nucl Phys B Proc Suppl 2003;125:60-8.
26. Ferrer L, Chouin N, Bitar A, Lisbona A, Bardiès M. Implementing dosimetry in GATE: Dose-point kernel validation with GEANT4 4.8.1. Cancer Biother Radiopharm 2007;22:125-9.
27. Jan S, Santin G, Strul D, Staelens S, Assié K, Autret D, *et al.* GATE: A simulation toolkit for PET and SPECT. Phys Med Biol 2004;49:4543-61.
28. Sarrut D, Bardiès M, Boussion N, Freud N, Jan S, Létang JM, *et al*. A review of the use and potential of the GATE Monte Carlo simulation code for radiation therapy and dosimetry applications. Med Phys 2014;41:064301.
29. Erdi YE, Wessels BW, Loew MH, Erdi AK. Threshold estimation in single photon emission computed tomography and planar imaging for clinical radioimmunotherapy. Cancer Res 1995;55:5823s-6.
30. Siegel JA, Thomas SR, Stubbs JB, Stabin MG, Hays MT, Koral KF, *et al.* MIRD pamphlet no. 16: Techniques for quantitative radiopharmaceutical biodistribution data acquisition and analysis for use in human radiation dose estimates. J Nucl Med 1999;40:37S-61.
31. Willowson K, Bailey DL, Baldock C. Quantitative SPECT reconstruction using CT-derived corrections. Phys Med Biol 2008;53:3099-112.

32. Plyku D, Hobbs R, Huang K, Atkins F, Garcia C, Sgouros G, *et al*. 124I-PET/CT based tumor dosimetry for 131I therapy of metastatic differentiated thyroid cancer (DTC) – A comparison of recombinant human thyroid-stimulating hormone vs thyroid hormone withdrawal patient preparation methods. J Nucl Med 2015;56:394.
33. Bolch WE, Eckerman KF, Sgouros G, Thomas SR. MIRD pamphlet No. 21: A generalized schema for radiopharmaceutical dosimetry – Standardization of nomenclature. J Nucl Med 2009;50:477-84.
34. Parach AA, Rajabi H, Tajik-Mansoury MA, Ahangari HT. Comparison of GATE and MCNP Monte Carlo codes for internal dosimetery. Iran J Nucl Med 2010;18:108.
35. Grimes J, Celler A. Comparison of internal dose estimates obtained using organ-level, voxel S value, and Monte Carlo techniques. Med Phys 2014;41:092501.
36. Sgouros G, Squeri S, Ballangrud AM, Kolbert KS, Teitcher JB, Panageas KS, *et al.* Patient-specific, 3-dimensional dosimetry in non-Hodgkin's lymphoma patients treated with 131I-anti-B1 antibody: Assessment of tumor dose-response. J Nucl Med 2003;44:260-8.
37. Rajendran JG, Fisher DR, Gopal AK, Durack LD, Press OW, Eary JF. High-dose (131) I-tositumomab (anti-CD20) radioimmunotherapy for non-Hodgkin's lymphoma: Adjusting radiation absorbed dose to actual organ volumes. J Nucl Med 2004;45:1059-64.
38. Sandström M, Garske-Román U, Johansson S, Granberg D, Sundin A, Freedman N. Kidney dosimetry during 177Lu-DOTATATE therapy in patients with neuroendocrine tumors: Aspects on calculation and tolerance. Acta Oncol 2018;57:516-21.
39. Divoli A, Chiavassa S, Ferrer L, Barbet J, Flux GD, Bardiès M. Effect of patient morphology on dosimetric calculations for internal irradiation as assessed by comparisons of Monte Carlo versus conventional methodologies. J Nucl Med 2009;50:316-23.
40. Pandit-Taskar N, Zanzonico P, Hilden P, Ostrovnaya I, Carrasquillo JA, Modak S. Assessment of organ dosimetry for planning repeat treatments of high-dose 131I-MIBG therapy: 123I-MIBG vs. post-therapy 131I-MIBG imaging. Clin Nucl Med 2017;42:741-8.
41. Kolbert KS, Pentlow KS, Pearson JR, Sheikh A, Finn RD, Humm JL, *et al.* Prediction of absorbed dose to normal organs in thyroid cancer patients treated with 131I by use of 124I PET and 3-dimensional internal dosimetry software. J Nucl Med 2007;48:143-9.
42. Kolbert KS, Sgouros G, Scott AM, Bronstein JE, Malane RA, Zhang J, *et al.* Implementation and evaluation of patient-specific three-dimensional internal dosimetry. J Nucl Med 1997;38:301-7.